

## Imaging compaction of single supercoiled DNA molecules by atomic force microscopy

Olga Y. Limanskaya<sup>1,2</sup> and Alex P. Limanskii<sup>1</sup>

<sup>1</sup> Department of New Infectious Diseases, Institute of Microbiology and Immunology, Ukrainian Academy of Medical Sciences, Pushkinskaya St. 14, 61057 Kharkov, Ukraine

<sup>2</sup> National Scientific Center – Institute of Experimental and Clinical Veterinary Medicine, Pushkinskaya St. 83, 61023 Kharkov, Ukraine

**Abstract.** Supercoiled pGEMEX DNA, 3993 bp in length, was immobilized on different substrates (freshly cleaved mica, standard amino mica and modified amino mica with increased hydrophobicity and surface charge density compared with standard amino mica) and was visualized by atomic force microscopy (AFM) in air. Plectonemically supercoiled DNA (scDNA) molecules, as well as extremely compacted single molecules, were visualized on amino-modified mica, characterized by increased hydrophobicity and surface charge density. We show four-fold increase in DNA folding on the mica surface with high positive charge density. This result is consistent with a strongly enhanced molecular flexibility facilitated by shielding of the DNA phosphate charges. The formation of minitoroids with about a 50 nm diameter and molecules in spherical conformation was the final stage of single molecule compaction. A possible model of conformational transitions for scDNA *in vitro* in the absence of protein is proposed based on AFM image analysis. Compaction of the single scDNA molecules, up to minitoroids and spheroids, appears to be caused by screening of the negatively charged DNA phosphate groups. The high surface charge density from positively charged amino groups on mica, on which DNA molecules were immobilized, is an obvious candidate for the screening effect.

**Key words:** DNA compaction — Supercoiled DNA — Amino mica — Atomic force microscopy

### Introduction

Extensive lengths (millimeters to meters) of genomic DNA is compacted by proteins, natural polyamines and other compounds. The resulting highly ordered structures appear in the nucleoids of prokaryotes and eukaryotic nuclei for which volumes range from several cubic to several hundred micrometers (Kim et al. 2004). The nucleoid volume of *Escherichia coli*, for instance, is nearly one fourth of the cell volume. A randomly packed DNA molecule without proteins occupies a much larger volume than that in the nucleus or in the bacterial cell (Grosberg and Khokhlov 1989). According to the current literature, DNA compaction in eukaryotes is caused by its interaction with

nuclear proteins, firstly with topoisomerases and histones to form nucleosomes, then with chromatin fibers to form chromosomes (Hizume et al. 2002; Yoshimura et al. 2002; Gonzalez-Huici et al. 2004). *In vivo* histone proteins neutralize approximately 57% of the electronegative sites associated with DNA charge (Morgan et al. 1987). The remaining DNA charge is neutralized by other cationic compounds, including natural polyamines, mono- and polyvalent cations, where cations make up to 1% of the cell weight (Zinchenko and Yoshikawa 2005).

Approximately 10 histone-like proteins are known to participate in DNA compaction in prokaryotes, among which DNA-binding proteins termed heat unstable, histone-like nucleoid structuring, integration host factor have been widely studied (Zimmerman 2004). The high-mobility group proteins are other DNA-binding proteins that modulate DNA-histone binding by interacting with DNA through sequence specific binding. The structural maintenance of chromosome group is nonhistone proteins including con-

Correspondence to: Alex P. Limanskii, Department of New Infectious Diseases, Institute of Microbiology and Immunology, Pushkinskaya St. 14, 61057 Kharkov, Ukraine  
E-mail: o.lymunskiy@mail.ru

densins and cohesins that have been identified as members of ATPase family. These proteins have been shown to play the central role in DNA compaction and their presence directly results in DNA condensation (Kemura et al. 1999).

Different model systems are used to investigate genomic architecture in the eukaryotic nucleus. The study of *E. coli* nucleoid by atomic force microscopy (AFM) has demonstrated that its structure changes during the cell cycle. Nucleoids in the stationary phase were found to be more tightly compacted than those in the log phase. For both cell phases, a common fibrous structure with a diameter of around 80 nm was identified as a fundamental nucleoidic unit. Additionally, thinner fibres with a diameter approximately 40 nm and a higher order loop were observed for nucleoids in the log phase (Kim et al. 2004).

The nucleosome, as the main repetitive unit of chromatin, is used as another model system. The well-known "beads-on-a-string" structure has been visualized for linear DNA complexes in which the histone octamer is formed by two molecules each containing H2A, H2B, H3 and H4 proteins (Sato et al. 1999).

Interestingly, the compaction and DNA condensation in toroidal and fibrous structures can be attained under conditions other than those well described for complex formation with proteins (Martinkina et al. 1998, 2000). Several groups have shown that different types of polycations (polylysine, protamine, cobalt hexamine), natural (spermidine<sup>3+</sup>, spermine<sup>4+</sup>) and synthetic polyamines (diaminopropane<sup>2+</sup>) induce DNA condensation and toroid formation (Allen et al. 1997; Bloomfield 1997; Dunlap et al. 1997; Golan et al. 1999). Moreover, DNA condensation can be observed without proteins and water-soluble multivalent cations. DNA molecules compact after immobilization on the positively charged surface of amino-coated mica (Fang and Hoh 1998a). Recent results have shown that the level of DNA condensation can be controlled by varying the valency of silanes used for mica modification as well as NaCl concentration during DNA immobilization (Fang and Hoh 1998a; Cherny and Jovin 2001). However, other than toroids, highly compacted DNA molecules were not visualized by varying NaCl concentration over a small range (10–100 mmol/l). Importantly, the study of linear DNA condensation has shown that multimolecular aggregates were formed by few DNA molecules and none by single molecules (Lin et al. 1998; Hud and Downing 2001).

DNA condensation up to and including nanoparticles size is a fundamental biological phenomenon that plays an important role during DNA packaging for viruses, prokaryotic nucleoids, eukaryotic nuclei as well as the development of nonviral methods for the delivery of genetic material.

This report provides AFM images of single supercoiled DNA (scDNA) molecules with a greater compaction

level than obtained in previous studies (Boles et al. 1990; Dunlap et al. 1997; Fang and Hoh 1998a,b, 1999; Cherny and Jovin 2001; Umemura et al. 2001; Bussiek et al. 2003). A modified amino mica, with the increased surface charge density compared with the standard amino mica, was used as a novel substrate for DNA immobilization. Different stages of molecular compaction for single circular DNA were observed with the new substrate. The length of the superhelical axis was observed to be two-four times less, corresponding to second and third order superhelical axes, respectively. Further, compaction of single scDNA molecules up to the level of rods, toroids, minitoroids and spheroids was observed.

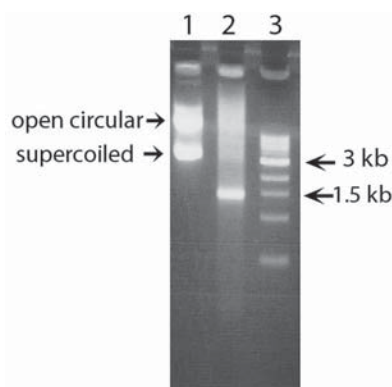
## Materials and Methods

### *Sample preparation and substrate modification for AFM*

Chemicals were purchased from Aldrich (USA) and Wakenyaku (Japan). Freshly cleaved mica, standard amino mica and modified amino mica with increased charge density were used as AFM substrates. HEPES buffer (10 mmol/l, pH 7.4) with MgCl<sub>2</sub> (2.5 mmol/l) was used for deposition of DNA onto freshly cleaved mica. A drop (10 µl) of DNA solution with (~ 0.01–0.1 µg/ml) in TE buffer (10 mmol/l Tris-HCl, pH 7.9; 1 mmol/l EDTA) was deposited onto a strip (1 cm<sup>2</sup>) of the standard or modified amino mica. Following incubation (2 min), the sample was rinsed with ultrapure water, carefully blown dry (in Ar vapor) and kept at reduced pressure (P = 100 mm Hg, 20 min). The standard amino mica was obtained according to the literature (Limansky et al. 2002) by silanation of freshly cleaved mica in distilled (3-aminopropyl) triethoxysilane (APTES) and N,N-diisopropyl ethylamine (Aldrich) vapors. The APTES was distilled at reduced pressure in Ar vapour. For mica amino modification, freshly cleaved mica was incubated in a desiccator (2.5 l) filled with APTES, N,N-diisopropyl ethylamine and Ar vapors (1 h). Modified amino mica with the increased charge density was obtained by a slightly modified procedure for standard amino mica silanation. Briefly, two-fold distilled APTES and longer incubation time comparing with time for standard amino mica (3 h instead of 1 h for standard amino mica) were applied. Modification of the preparation procedure results in increased hydrophobicity and surface charge density of mica because content of aqueous vapors is noticeably decreasing after twice distillation of APTES.

### *AFM*

Supercoiled pGEMEX DNA (Promega, USA), 3993 bp in length, was used for all studies (Fig. 1). A Nanoscope IV



**Figure 1.** Analysis of supercoiled and linear DNA by 2% agarose gel electrophoresis. Lane 1: supercoiled pGEMEX DNA of 3993 bp length; lane 2: 1.4 kb amplicon; lane 3: 1 kb ladder.

MultiMode atomic force microscope (Veeco Instruments Inc., USA) with E-scanner (maximal range 12  $\mu\text{m}$ ) was used for all experiments. All DNA images were captured using tapping mode AFM in air at room temperature with OMCL-AC160TS cantilevers (Olympus Optical Co., Japan; resonant frequency 340–360 kHz; nominal spring constant 42 N/m) at 3 Hz scan line speed. High resolution (512  $\times$  512 pixels) topography images were acquired simultaneously and were processed using the flattening function of the Nanoscope software (version 5.12r3; Veeco Instruments Inc., USA).

The apparent volume of individual DNA molecules was calculated from measurements (width and length) of AFM image features and their corresponding cross-section profiles (height and partial length). Longitudinal cross-sections of molecules were calculated using the Nanoscope software. DNA molecule was divided into several fragments, and cross-sectional profiles were built for every fragment. Number of these fragments ranged from 2 to 9 depending on the topology of the molecule. The apparent molecular volume of DNA was determined by multiplying the width of the molecule by the sum of squares determined from the longitudinal cross-sections. The full width of DNA molecule at half maximum was applied for these calculations.

Search of triplexes (homopurine-homopyrimidine mirror repeats) in the pGEMEX plasmid was performed by software GeneBee (Brodsky et al. 1991).

#### Sample preparation for PCR

For amplification by polymerase chain reaction (PCR), linear DNA templates were obtained from the restriction digestion of supercoiled pGEMEX DNA of 3993 bp length with endonuclease ScaI (New England Biolabs, England). The linear DNA was directly subjected to PCR to amplify the DNA fragment with a promoter and transcription

termination site for T7 RNA polymerase with a 1414 bp length. Sequences of the designed primers, L1 and L2, including their positions on the pGEMEX DNA are following: 5'-cgc tta caa ttt cca ttc gcc att c-3' sense primer L1 (3748–3772), 5'-ctg att ctg tgg ata acc gta tta ccg-3' reverse primer L2 (1168–1142).


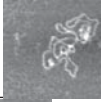
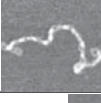

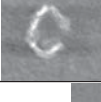
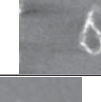





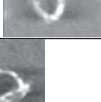

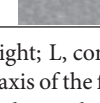
Oligonucleotides (Sigma, USA) were used for hot start PCRs (50  $\mu\text{l}$  volume) in a thermal cycler (GeneAmp 9700, Perkin Elmer, USA). For PCRs, two types of high fidelity Taq DNA polymerase were used. The reaction mixture contained 2.5 units of Pyrobest DNA polymerase (TaKaRa Co., Japan) or Invitrogen Platinum DNA polymerase (Invitrogen, Japan) as well as buffer concentrate (2.5 mmol/l  $\text{MgCl}_2$ , 0.2 mmol/l dNTP mixture), two primers (1  $\mu\text{mol/l}$  of each) and DNA template (approximately 0.01  $\mu\text{g}$ ). Thermal cycling was comprised of an initial incubation (95°C; 4 min), 35 cycles of denaturation (95°C, 1 min), primer annealing (69–73°C; 1 min), and extension (74°C, 2 min). Several PCRs were performed at different annealing temperatures (69, 71 and 73°C) to minimize unspecific PCR products. Amplicons were visualized and separated by running amplified mixture (10  $\mu\text{l}$ ) on TAE agarose gel (2% (v/v)), followed by ethidium bromide staining (Fig. 1). The band of the expected PCR product length was excised from the agarose gel using a long-wave low intensity UV lamp (BioRad, USA) and purified with a QIAquick PCR purification kit (QIAGEN, Japan) followed by phenol/chloroform extraction and ethanol precipitation.

## Results

The length of the superhelical axis for 3.5 kb scDNA was constant for a range ( $0.03 < |\sigma| < 0.12$ ) of the superhelical density, and is approximately 35% of the contour length of the relaxed molecule (Boles et al. 1990). This relationship is appropriate for ~4 kb supercoiled pGEMEX DNA molecules immobilized onto freshly cleaved mica with a relatively low surface charge density and hydrophobicity (Table 1, position A3).

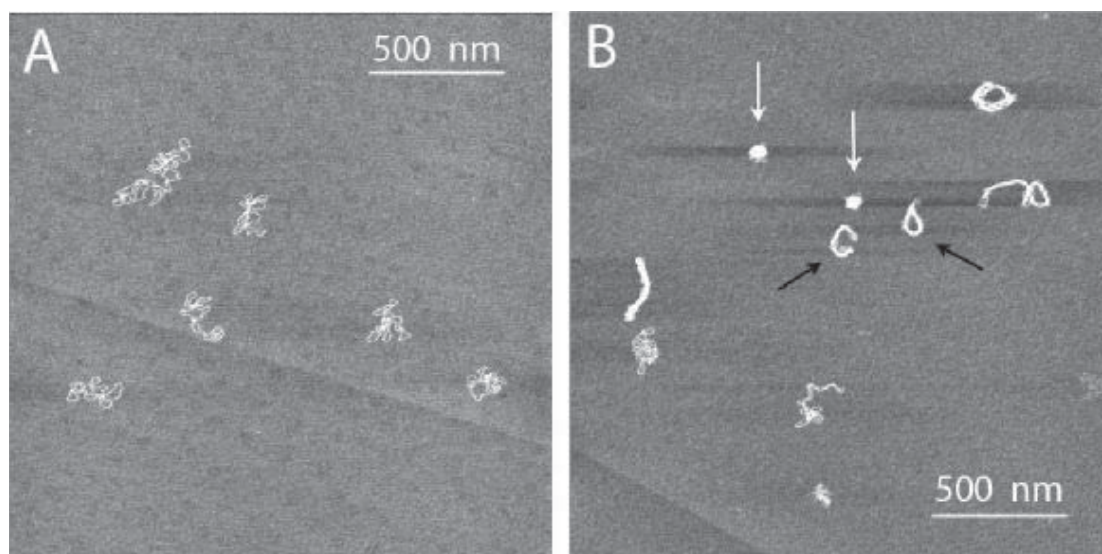
There was significant DNA compaction accompanied by a decreasing length of the superhelical axis following immobilization of supercoiled circular DNA on the modified amino mica with increased surface charge density and hydrophobicity (Fig. 2). For 108 individual molecules studied, typical variants for 98 single scDNA molecules with corresponding parameters are described in Table 1. The remaining 10 molecules represent intermediate variants of the condensed molecules. The number of plectonemically scDNA molecules with a low superhelical density ( $\sigma \sim -0.024$ , A2 in Table 1) makes up 21% of the scDNA molecules with a high superhelical density ( $\sigma \sim -0.13$ ) and there were 12% of those forming a superhelical axis of the first order (B3 in Table 1). There were 27% scDNA with second order

**Table 1.** Parameters of supercoiled pGEMEX DNA molecules which were determined from AFM images. Theoretical excluded volume value for pGEMEX DNA in B-form is  $V = 4010 \text{ nm}^3$ . The numbers in the first column correspond to positions in Fig. 7; number of similar visualized molecules is indicated in parenthesis

No.	Molecule(s)	$h_{\max}$ (nm)	$h_{\min}$ (nm)	L (nm)	l (nm)	V ( $\text{nm}^3$ )
A3 <sup>d</sup> (3)		0.80	0.35 <sup>*</sup>	1243	46 <sup>a</sup>	3510
A2 <sup>e</sup> (21)		0.99	0.35 <sup>*</sup>	1216	–	3530
B3 (12)		0.95	0.35 <sup>*</sup>	567	567 <sup>a</sup>	4440
C3 (16)		1.69	0.78	279	279 <sup>b</sup>	3280
B2 (4)		1.35	0.28 <sup>*</sup>	260	260 <sup>b</sup>	3470
C2 (7)		1.36	0.30 <sup>*</sup>	270	270 <sup>b</sup>	3520
D2 (3)		3.00	1.25	140	140 <sup>c</sup>	5180
D3 (7)		1.74	0.84	260	260	3980
E2 (4)		2.60	1.85	–	–	3620
F2 (17)		3.45	0.30 <sup>*</sup>	–	–	3140
B1 (1)		1.40	0.35 <sup>*</sup>	548	548	6300
E1 (1)		2.00	0.87	269	269 <sup>b</sup>	7080
C1 (1)		2.00	0.45 <sup>*</sup>	–	401	6840
D1 (1)		2.10	0.30 <sup>*</sup>	267	267	6570

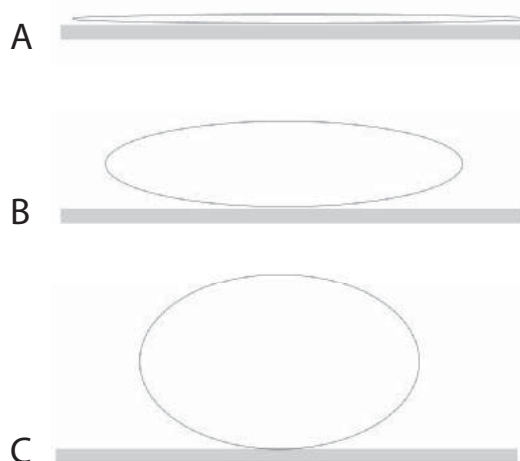
$h_{\max}$ , maximal height;  $h_{\min}$ , minimal height; L, contour length of supercoiled molecule; l, length of superhelical axis; V, apparent volume; <sup>\*</sup> double-stranded DNA; <sup>a</sup> superhelical axis of the first order; <sup>b</sup> superhelical axis of the second order; <sup>c</sup> superhelical axis of the third order; <sup>d</sup> DNA was immobilized from buffer with  $\text{MgCl}_2$  on the freshly cleaved mica; <sup>e</sup> DNA was immobilized on standard amino mica.





**Figure 2.** AFM image of supercoiled pGEMEX DNA with length of 3993 bp after deposition of DNA solution in TE buffer onto standard amino mica (A) and modified amino mica surface (B) which is characterized by higher hydrophobicity and surface density of amino groups, i.e. increased charge density as compared with standard amino mica. Scan size is  $2 \times 2 \mu\text{m}$ . Supercoiled molecules of different topology are shown: from plectonemically supercoiled (A) to supercoiled molecules with different length of superhelical axis (B). Vertical white arrows indicate scDNA molecules in spherical conformation; black tilted arrows show molecules in toroidal conformation and in close topology to toroidal conformation.

(C3, B2 and C2 in Table 1), 14% with third order (positions D2, D3 and E2 in Table 1) superhelical axes and 17% highly compacted single DNA molecules, i.e. so-called spheroids (position E3 in Table 1).



**Figure 3.** Drop of DNA solution after deposition on the mica surface with different hydrophobicity. **A.** Hydrophilic freshly cleaved mica surface. **B.** Hydrophobic standard amino mica. **C.** Modified amino mica with higher hydrophobicity and surface charge density as compared with standard amino mica.

Amino-modified mica is made by exposing mica to vapors of amino silane derivative. This type of AFM substrate is widely used, but its physical and chemical properties are poorly understood and investigated with only approximate estimations of amino group surface density (standard amino mica has  $\sim 1$  amino group per  $10^4 \text{ \AA}^2$ ). Furthermore, the standard amino mica can be considered as a polycation, but only 50% of the surface amino groups are known to be active or protonated groups (Shlyakhtenko et al. 1999).

Here we estimate the density of amino groups on the silicon surface following amino silane APTES treatment, which in the first approximation can be considered a similar surface to mica. For the first amino variant, there is one amino group per  $1290 \text{ \AA}^2$  for every APTES molecule that interacts with three OH-groups on Si surface (Reiner et al. 2003). On the contrary, silicon nitride (i.e. composition of certain AFM probes) exposed to APTES vapours exhibits  $1730 \pm 200$  amino groups per  $1 \mu\text{m}^2$  (Reiner et al. 2003), corresponding to one amino ( $\text{NH}_2$ )-group per  $387 \text{ \AA}^2$ . This data suggests a one to one interaction between APTES molecule and OH-groups on the silicon surface and are in agreement with reported data (Korolev et al. 2003). This study has shown the binding of  $\text{NH}_3$  cation with DNA binding site excludes the binding of another cation with neighbour DNA binding site if the distance between neighbour sites is less than  $8 \text{ \AA}$ . This means that one binding site for polycations interacting with double-stranded DNA should be located at the distance of

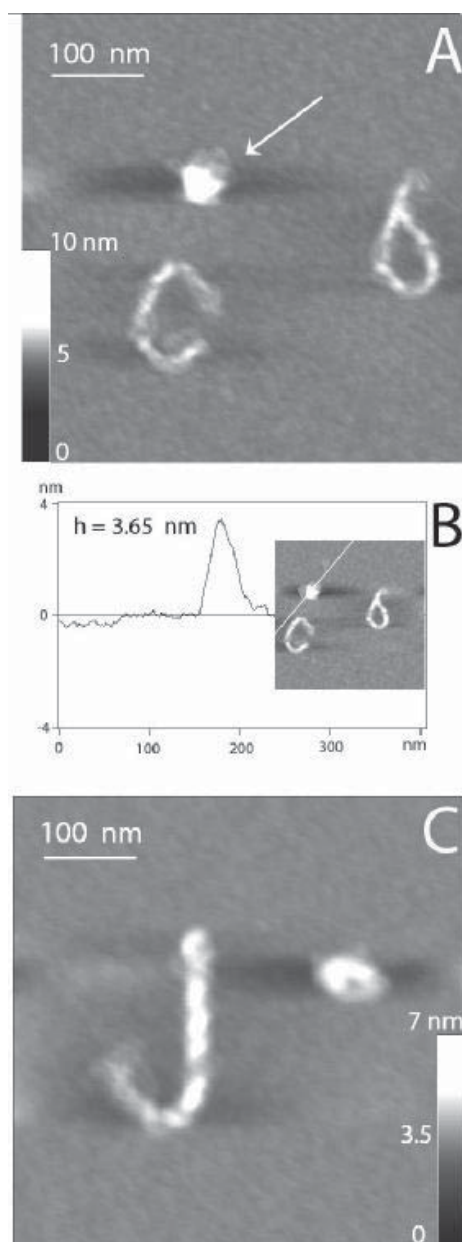
4 Å from another one. Korolev and co-workers determined the electronegative binding site of DNA to be  $251 \text{ \AA}^2$ . In this case, 42% of the negatively charged phosphate groups are neutralized upon interaction of the DNA with polycations, because the distance between binding sites is 4 Å along DNA axis if  $\text{NH}_3$  cations interact with all DNA binding sites.

Since the interaction between DNA and polycations is defined by ionic and hydrophobic interactions, the substrates studied in this paper can be arranged according to their increased hydrophobicity and surface positive charge density: freshly cleaved mica < standard amino mica < modified amino mica. This suggestion can be illustrated by a simple experiment (Fig. 3). A drop of aqueous solution deposited onto hydrophilic freshly cleaved mica spread out on the mica surface (Fig. 3A). Strikingly, a drop of the same solution deposited directly onto the standard amino mica surface adopted an elliptical form (Fig. 3B). However, a drop on a more hydrophobic surface of modified amino mica adopted an almost spherical conformation (Fig. 3C).

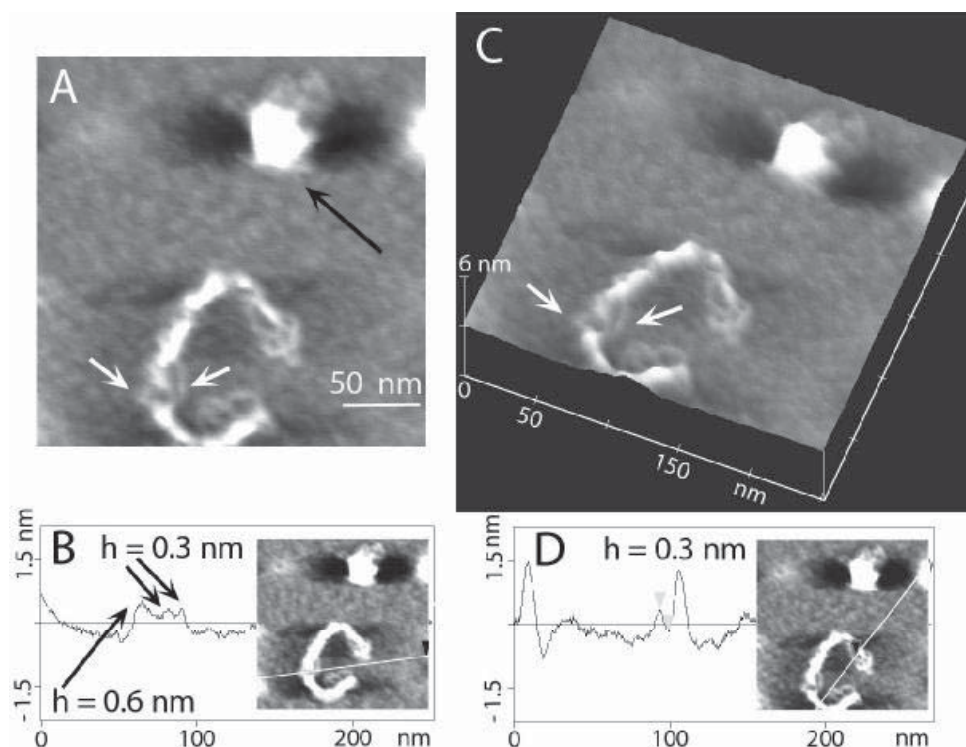
Note that surface properties of amino mica depend on several factors. For instance, we empirically determined that the standard amino mica for high quality DNA imaging can be obtained by treatment in vapors of distilled APTES under reduced pressure with an inert gas. Applying undistilled APTES (which is subjected to hydrolysis in air) produces amino mica with the low surface charge density and hydrophobicity, unsuitable as a DNA substrate for high quality AFM images.

The surface properties of amino mica (elasticity, charge) can be characterized by a variety methods, including X-ray photoelectron spectroscopy, Raman spectroscopy and AFM force measurements to determine the number of protonated amino groups and adhesion force, respectively. Previously, we determined that the adhesion force (2–4.6 nN) for the standard amino mica, i.e. force which is required for disengage surfaces of amino mica and AFM tip, in TE buffer for different probes (Lyman's'kiy and Lyman's'ka 2002). Further, it was determined that the topology of scDNA immobilized on the amino mica is the most sensitive parameter for the “quality” of the amino mica surface, since amino mica is used as a substrate for imaging linear and scDNA molecules.

Single scDNA molecules forming the superhelical axis of the second order are presented in Fig. 4A. The superhelical length of these highly compacted molecules is reduced (as compared with plectonemically scDNA) to the value 260 nm, i.e. approximately one fifth of the contour length of the relaxed DNA. Another type of highly compacted scDNA molecules formed on the surface of the modified amino mica is a spheroid (arrow in Fig. 4A). The cross-section profile of the spheroid for the determination of its excluded volume is shown in Fig. 4B. As a rule, we constructed a longitudinal cross-sectional profile of the molecule by the perpendicular plane to the mica plane instead of measuring the molecule height, which varies significantly for scDNA. This method gives a more precise calculation of the volume



**Figure 4.** **A.** AFM image of single supercoiled pGEMEX DNA molecules on the modified amino mica. Length of the superhelical axis of DNA (260–270 nm) is about one fifth the contour length of the relaxed molecule. Arrow indicates DNA molecule that was compacted up to the spheroid level. Scale corresponding to Z range from 0 to 10 nm is shown for the estimation of molecule height. Scan size is  $500 \times 500$  nm. **B.** Cross-section of DNA molecule in spherical conformation from which height ( $h_{\text{max}} = 3.65$  nm) and square of molecule cross-section were determined. The line of the cross-section is illustrated in the inset. **C.** AFM image of supercoiled pGEMEX DNA molecules that have formed dimer. Length of superhelical axis (260 nm) and dimer apparent volume is equal to two volumes of single scDNA molecules. Scan size is  $500 \times 500$  nm and the scale corresponds to a Z range from 0 to 7 nm. The semispheroid formed by single DNA molecules is located near the dimer.



**Figure 5.** AFM image (A), cross-sections (B and D) and three dimensional image of single supercoiled pGEMEX DNA molecule forming superhelical axis of second order (C). A. White arrows indicate separated chains, of which the cross-section is shown in Fig. 3B; and black arrow shows the spheroid. Scan size is  $250 \times 250$  nm. B. Cross-sectional profile of three separated chains. The height of two peaks (0.3 nm) is equal to the height of double-stranded DNA immobilized on mica, and the height of the third peak (0.6 nm) is double that. Line of cross-section is shown in inset. D. Cross-sectional profile of separated chain of another fragment. The height of the peak is 0.3 nm. The line of the cross-section is shown in the inset.

for the condensed structure. For instance, the height of nodes formed by two intertwined chains may increase (1.3–1.8 nm) compared with that for a DNA double helix immobilized on the mica (0.3–0.4 nm).

Based on the volume calculation for the condensed structure, we can determine the number of compacted scDNA molecules from which the condensed structure was formed. The value of apparent DNA volume can be calculated for microorganisms having a complete genome by multiplying the DNA diameter (2 nm) by the square of its cross-sectional profile, assuming B-DNA, i.e. for the distance between nucleotides along duplex axis  $H = 3.4$  Å. The volume of the spheroid in Fig. 4A ( $3140 \text{ nm}^3$ ) was calculated in this manner, indicating that the spheroid is formed by a single scDNA molecule. The comparison is made with the theoretically calculated apparent volume of pGEMEX DNA ( $4010 \text{ nm}^3$ ) also assuming B-DNA.

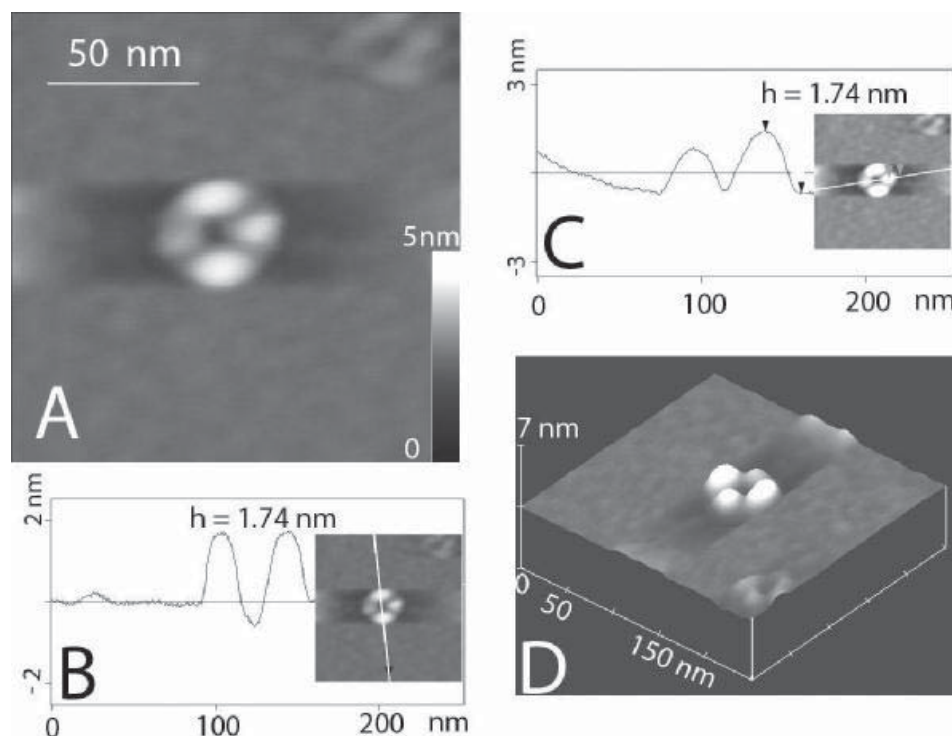
As a result of further compaction, molecules four times shorter in length of the superhelical axis (the length of the superhelical axis of the third order is 140 nm, position D2 in Table 1) and molecules in semispherical (position E2 in Table 1) and spherical (position F2 in Table 1) conformations are formed.

Compaction of molecules on the modified amino mica arises not only for single DNA molecules, but also for dimers (Fig. 4B). This compacted structure is characterized by an apparent volume ( $7080 \text{ nm}^3$ ) corresponding to formation by two scDNA molecules. The length of the dimer superhelical axis (260 nm) is similar to single scDNA molecule (Fig. 4A).

#### *Compacted structures are formed by single DNA molecules*

In recent studies (Hud and Downing 2001; Hizume et al. 2002), DNA condensation in the presence of different factors including proteins was demonstrated only for dimers and trimers, but not for single molecules. Therefore the C-like supercoiled molecule, which is in close to the toroidal conformation (Fig. 4A), requires further consideration. An AFM image of this molecule at higher resolution (Fig. 5A) in combination with the 3D-image (Fig. 5C) clearly shows that the scDNA molecule is formed by several distinctly discriminating strands (arrows indicate a fragment of the molecule with three locally separated strands). The cross-sectional profile (Fig. 5B) through these strands (line in inset shows the direction





**Figure 6.** AFM image (A), cross-sections (B and C) and 3D image (D) of toroid formed by single supercoiled pGEMEX DNA molecule. A. Scan size is  $250 \times 250$  nm. B. Cross-section height (1.74 nm) is shown for two toroid fragments. C. Height of other toroid fragments (1.74 and 0.84 nm) was determined from another cross-section. Triangles indicate peaks corresponding to toroid segment with height  $h = 1.74$  nm and background, respectively. A. and D. Outer diameter of minitoroid is 50–60 nm, inner diameter is 15–25 nm.

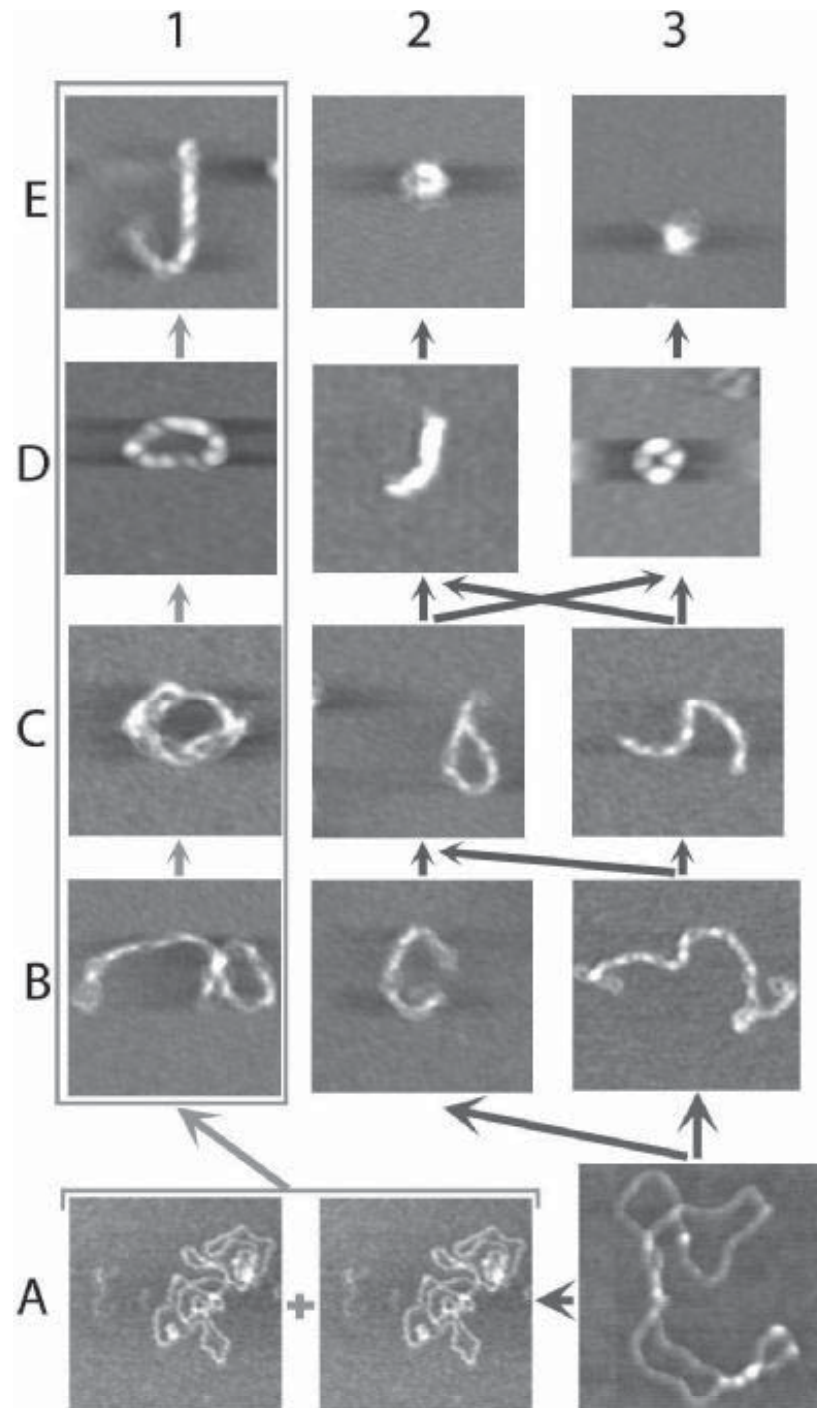
of the cross-section, perpendicular to the plane of the image) indicates their height. The ability to measure the height of a molecule immobilized on a substrate with subnanometer resolution is an important AFM capability, discriminating this method from electron microscopy. Given the height of both DNA strands (0.3 nm) and the third strand (0.6 nm), it appears that the two separate chains of this scDNA represent double-stranded DNA chains. The former height value is in agreement with literature data for the height of adsorbed DNA measured by AFM (Tanigawa and Okada 1998), while the latter corresponds to two intertwined double-stranded chains (i.e. the double height of double-stranded DNA immobilized on the mica). Finally, cross-sectional analysis shows that the C-like scDNA is formed by four double-stranded DNA chains. The contour length of the aforementioned scDNA (260 nm) indicates that the visualized compacted structure is formed by a single, circular DNA molecule folded in half. For a dimer with this contour length (260 nm), the cross-sectional profile should correspond to eight strands.

Another cross-sectional profile for a C-like molecule (Fig. 5D) confirms its formation from double-stranded DNA chains (0.3 nm). Taken together with a calculation of the apparent volume of the molecule also permits the differentiation of

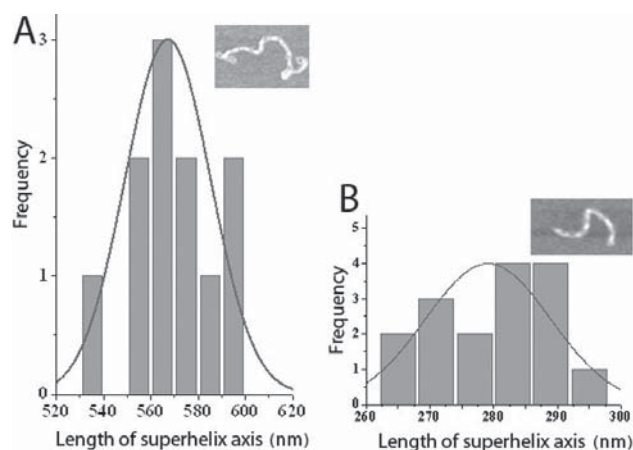
monomolecular structures from aggregates formed by several molecules. Attentive analysis of the AFM images of scDNA (e.g. Fig. 5A and Fig. 5C) shows the height of intertwined DNA chains forming scDNA to be equal to double the height of double-stranded DNA ( $h = 0.3$  nm), but only if chains are wound and closely touch each other. On the contrary, when chains are wound but do not touch each other closely, the height of such molecule can increase (1.3–1.8 nm).

Another supercoiled structure, the minitoroid, looks like a spheroid in the AFM image at low resolution. Cross-sections and a 3D image of a minitoroid, formed from single scDNA, are shown in Fig. 6. The apparent volume of this molecule ( $3980 \text{ nm}^3$ ) corresponds to that of the single pGEMEX DNA molecule. From cross-sections (Fig. 6B and 6C), we determined that three of four toroidal segments have the same height (1.74 nm) and the height of the fourth segment is two times less (0.84 nm). This means that in the fourth segment of the toroid, the number of coils formed by scDNA is less than the other three segments. The toroid appears as a minicircle with a gap in the upper part and length one fourth that of the toroidal circle length. This minitoroid feature indicates that toroidal molecules may be formed by the bending of rod-like molecules. Similar results were





**Figure 7.** Compaction model of scDNA molecules proposed from the analysis of AFM images for supercoiled pGEMEX DNA. A1, A2 – standard amino mica; A3 – freshly cleaved mica, all other images were captured for modified amino mica. Arrows indicate possible mods of further DNA compaction. Different topological variants of compacted DNA molecules are forming at increasing hydrophobicity and surface charge density (density of protonated amino groups), or the transition from freshly cleaved mica and standard amino mica to modified amino mica. B3 – scDNA forming a superhelical axis of the first order and contour length of the compacted molecule is equal to about half that of relaxed molecule; B2, C2, C3 – scDNA with superhelical axis of second order and contour length of compacted molecule is equal to about one fifth the contour length of the relaxed molecule; D2 – scDNA with superhelical axis of third order (contour length of compacted molecule is equal one eighth contour length of relaxed molecule); E2, E3 – spheroids; D3 – minitoroid formed by single DNA molecule. Four dimers are marked by rectangle. B1, C1, D1 – condensed structures which were formed by two DNA molecules.



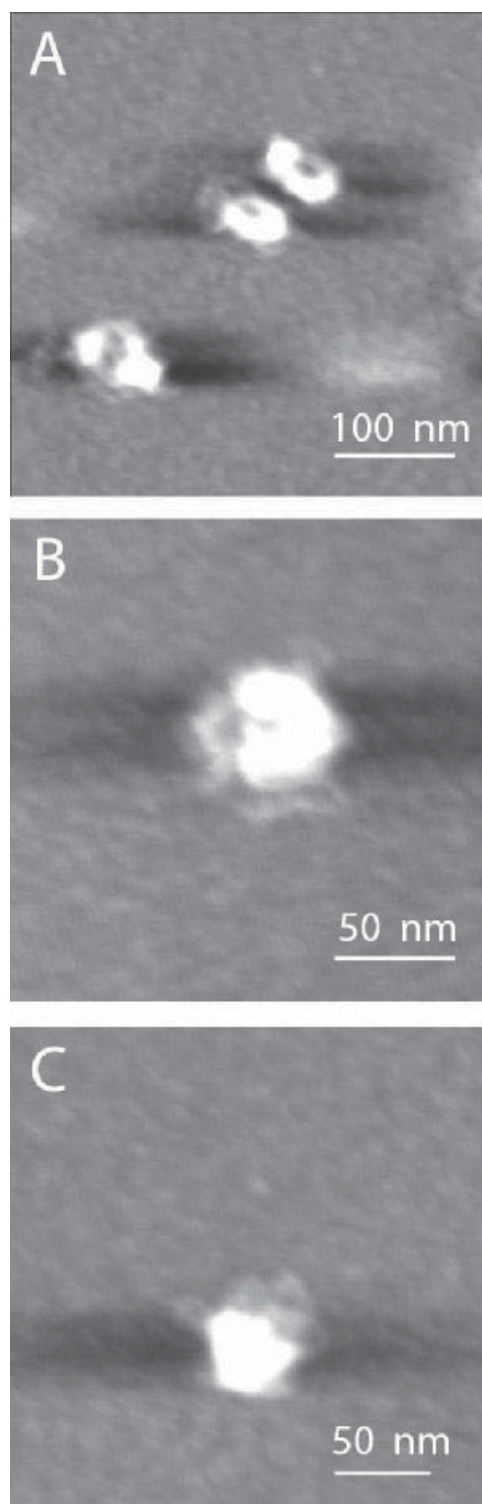
**Figure 8.** Determined from AFM images, length of superhelical axis of scDNA molecules forming superhelical axes of second (A) and third (B) order. Lengths of superhelical axis are  $567 \pm 18$  nm and  $279 \pm 10$  nm, respectively. Lines represent normal distributions. Inserts show typical AFM images of scDNA taken for statistical analysis.

obtained for toroids formed by several long linear phage  $\lambda$  DNA (Lin et al. 1998).

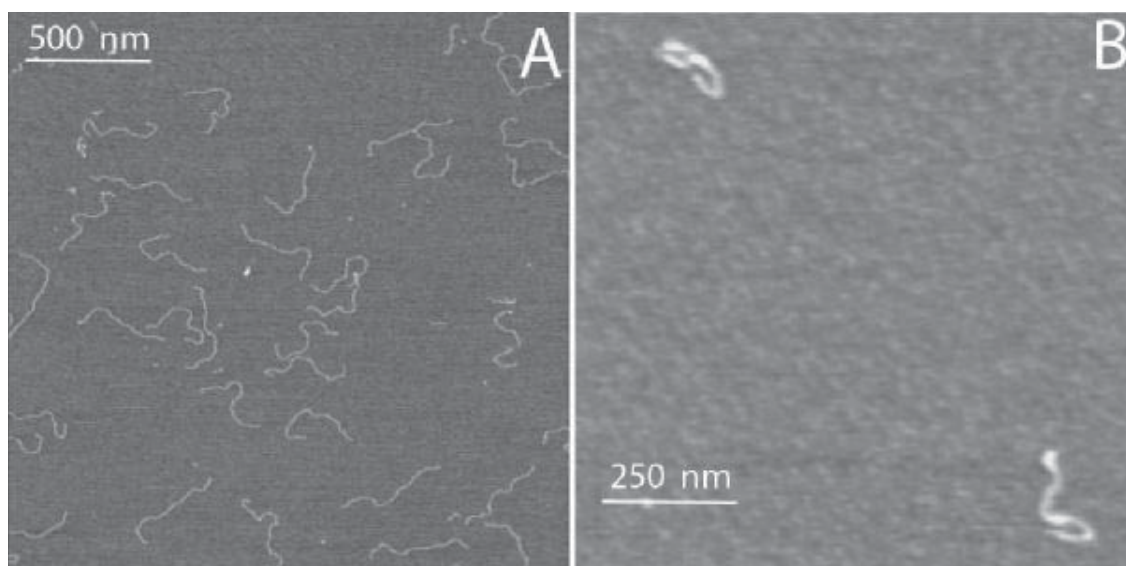
In general, previous studies have shown that toroidal structures are formed by several linear or circular DNA molecules (Fang and Hoh 1998b; Hansma et al. 1998; Lin et al. 1998; Golan et al 1999). We also visualized toroids formed from two scDNA molecules. Parameters of several toroids are given in Table 1. Positions C1 and D1 correspond to toroids formed by two DNA molecules since the volume of these condensed assemblies is equal to double volume of single supercoiled pGEMEX DNA. Parameters and AFM images of single DNA molecules are presented in Table 1 for all other positions, excluding the position E1 that corresponds to a dimeric rod.

*Molecules with second and third order superhelical axes give rise to compaction of scDNA molecules*

Based on the analysis of the AFM images, we propose a model for the compaction of single DNA molecules and dimers (Fig. 7). Positions B1, C1, D1, E1, marked by the rectangle, correspond to dimers of scDNA as determined from the apparent volume measurements; while all other positions indicate single molecules. Molecules with low compaction are shown in positions A1-A3, and molecules with the highest compaction level are found in E1-E3. Supercoiled pGEMEX DNA immobilized on the freshly cleaved mica (characterized by low surface charge density) from buffer solution with  $Mg^{2+}$  ions (position A3) has superhelical nodes (7–8) and superhelical density ( $-0.024$ ). Supercoiled pGEMEX DNA molecules immobilized on the standard amino mica (posi-



**Figure 9.** AFM images of compacted supercoiled pGEMEX DNA molecules. A. Three minitoroids are formed by three single DNA molecules. Scan size is  $400 \times 400$  nm. B. Semispheroid ( $h_{max} = 2.6$  nm) is compared to the height of the uncompacted DNA chain ( $h_{min} = 0.3$  nm) that is consistent with double-stranded DNA. C. Spheroid ( $h_{max} = 3.45$  nm). Scan size is  $250 \times 250$  nm.



**Figure 10.** AFM image of an amplified fragment of pGEMEX DNA. **A.** Freshly cleaved mica. Scan size is  $2.2 \times 2.2 \mu\text{m}$ . Expected amplicon contour length (485 nm) suggests B-DNA. Measured contour length of amplicon ( $435 \pm 15 \text{ nm}$ ) corresponds to a distance of  $3.07 \text{ \AA}$  between nucleotides along the double stranded helix axis. **B.** Modified amino mica with increased surface charge density (i.e. density of protonated aminogroups). Scan size is  $1 \times 1 \mu\text{m}$ . Amplicon contour length ( $296 \pm 14 \text{ nm}$ ) is consistent with a  $2.09 \text{ \AA}$  distance between nucleotides along the duplex axis.

tions A1, A2), having a higher surface charge density and hydrophobicity compared to freshly cleaved mica, appear quite different. These molecules also appear as plectonemically scDNA molecules, but are more compacted and are localized in a smaller substrate area.

At the transition to modified amino mica (all other AFM images are obtained for this type of the substrate), which is characterized by a significantly higher surface charge density and hydrophobicity compared to standard amino mica, there were several types of compacted scDNA molecules. During the first stage of compaction, a number of nodes increase and scDNA molecules (position B3 in Fig. 7) with rod-like structures formed. In the latter case, the length of the superhelical axis is about half of the contour length of the relaxed molecule. The length distribution of the superhelical axis for this type of scDNA molecules is shown in Fig. 8A. Similar histograms were obtained for other topologically discriminating variants of compacted DNA molecules, and the accuracy of length measurements is about 13%. The length of the superhelical axis ( $567 \pm 18 \text{ nm}$ ) for the molecule indicated in Fig. 8A is very close to the length of the superhelical axis for plectonemically scDNA molecule. However, the number of nodes was significantly increased and, as a consequence, the superhelical density was increased ( $-0.13$ ).

At the second stage, these rod-like molecules are folded in half, i.e. the length of the superhelical axis is two-fold reduced (Fig. 8B), approximately equal to one fifth of the contour length of the relaxed molecule (C3, B2, C2 in

Table 1). Also at this stage, the rods fold further (C3) and toroids assemble (C2). At the third stage, shorter rods having a two-fold smaller superhelical axis length (140 nm) are able to fold (D2). Further, the formation of minitoroids (D3) from toroidal (C2) or rod-like (C3) molecules is possible. In the fourth stage, a further compaction of the toroids and rods results in the folding of semispheroids (E2) and spheroids (E3).

AFM images of these highly compacted molecules are shown in Fig. 9. It is important that these minitoroids are located as groups of molecules (Fig. 9A) or as a single structure (Fig. 6A). Towards answering the question of why different DNA molecules are compacted up to various levels, we suggest that: i) protonated amino groups on the modified amino mica surface are immobilized ununiformly, ii) spheroids and semispheroids are assembled on the fragments of modified amino mica with the maximal density of active amino groups. The location of topologically closed scDNA forms (minitoroids, rod-like molecules superhelical axis lengths of 570 nm and 280 nm) on small areas ( $500 \times 500 \text{ nm}$ ) of the mica demonstrates that the surface density of amino modified mica is varied. This surface charge gradient allows for variable screening of DNA phosphate groups and, consequently, the formation of morphologically different variants of compacted scDNA molecules. Furthermore, the DNA samples used herein contain topoisomers with different superhelical densities. The characteristic time of DNA compaction corresponds

to the time of DNA immobilization from solution onto the mica surface, giving rise to condensation of aggregates with different levels of compaction, such as topoisomers with different numbers of supercoils.

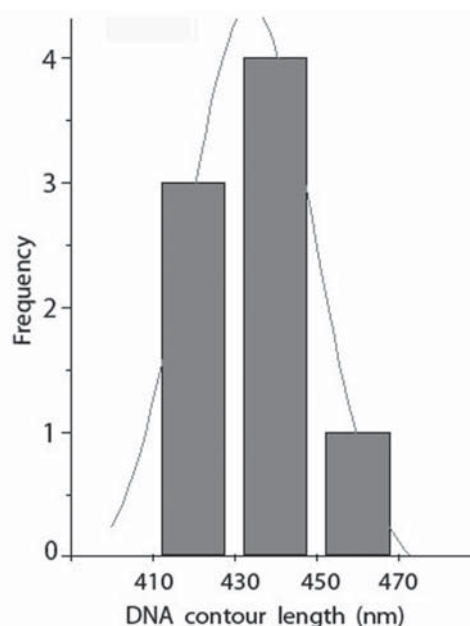
Another type of scDNA compaction corresponds to dimers instead of single molecules. Structures from AFM images (B1, C1, D1, E1) are formed by dimers, as concluded from their apparent volume values. First, two plectonemically scDNA molecules (A1, A2) form the rod-like structure (B1). This is followed by the formation of toroids (C1, D1) or rods (E1) with superhelical axis lengths approximately of one fifth that of relaxed molecules. Position D2 shows a toroid formed by two scDNA molecules.

#### Compaction mechanism of scDNA

Plectonemically scDNA molecules with low superhelical density are observed in AFM images (position A1 in Table 1) from samples prepared by immobilizing pGEMEX DNA molecules from buffer (with  $Mg^{2+}$  ions) onto the surface of the freshly cleaved mica. In previous reports focusing on the mechanism of DNA condensation by different proteins (histones, condensins) and using various model systems, including nucleosomes, highly compacted DNA molecules have not been visualized (Kemura et al. 1999; Hizume et al. 2002; Yoshimura et al. 2002). The latter discrepancy likely results from the use of freshly cleaved mica with  $Mg^{2+}$  ions characterized by low-surface charge density. Moreover, like  $Ca^{2+}$  ions,  $Mg^{2+}$  ions may interfere with scDNA compaction. Indeed, interference of  $Ca^{2+}$  ions with DNA compaction for the DNA complex with histone protein HMGB1 was reported previously (Polyanichko et al. 2002).

We modeled processes of DNA supercoiling and compaction using a circular plastic tube. It was expected that with the increase in supercoil number and upon the formation of superhelical axes of the second and third orders (i.e. at folding rod-like molecules in two and four times), the total tension and curved rigidity of compacted molecules would increase. However, with a small decrease in mechanical tension in the rod but constant maximal supercoils (nodes), the rod was transformed into a toroidal molecule. On the other hand, the conformational flexibility of scDNA was reported to increase during its interaction with histone proteins as for the formation of tetrasome, nucleosome and chromatosome (Sivolob and Prunell 2004). The significant increase in DNA conformational flexibility was explained by the increase in the DNA superhelical radius, possibly a requirement for the function of nucleosomal DNA in chromatin.

To more carefully elucidate the mechanism of DNA compaction and taking into consideration the decrease in the contour length for linear DNA from its immobilization onto



**Figure 11.** Distribution of amplicon contour length following the PCR and following purification as calculated from AFM images of DNA immobilized onto freshly cleaved mica. Line indicates Gaussian fit of the distribution.

mica with low surface charge density (Rivetti et al. 2003), we performed a preliminary study of the compaction of linear DNA molecules. For this purpose, linear DNA (1414 bp) was immobilized on freshly cleaved mica (Fig. 10A) and modified amino mica (Fig. 10B). The contour length of the molecules was determined directly from the AFM images. The contour length ( $435 \pm 15$  nm) for molecules immobilized on the freshly cleaved mica (Fig. 11) corresponded to a helical rise per bp of  $3.10 \text{ \AA}$ , within the range for B-DNA ( $3.03 \text{ \AA} < H < 3.37 \text{ \AA}$ ) and for A-DNA ( $2.56 \text{ \AA} < H < 3.29 \text{ \AA}$ ) (Saenger 1987). The contour length ( $296 \pm 14$  nm) of amplicon immobilized on the modified amino mica was equal to that of the distance between base pairs along the duplex axis ( $2.09 \text{ \AA}$ ). These results indicate that linear DNA immobilized on modified amino mica can be compacted as a result of surface properties.

We used the same procedure for the preparation of sample for the modified and standard amino mica, on that only plectonemically scDNA molecules were visualized and highly compacted structures were absent. This means that the compaction of DNA molecules occurs under the influence of surface properties of modified amino mica. We suppose that the compaction of scDNA molecules in solution occurs near the amino mica surface, because, in this case, both the conformational mobility of molecules and a high level of shielding of DNA phosphate groups necessary for compaction are provided.



## Discussion

Despite a great number of experimental studies of the DNA interaction with multivalent cations, the experimental and theoretical aspects of this phenomenon were investigated insufficiently. Even small polyamines cannot be represented as simple point ions, as assumed in classical theories of polyelectrolytes, e.g., in the condensation theory of Manning (1978) and the Poisson-Boltzmann theory (Anderson and Record 1995). The Manning condensation theory, which predicts the direct relationship between the neutralization of DNA charge and the concentration of mono- and multivalent ions and which was preferred in the 1970–1980s, states that about 90% of the negative charge of phosphate groups should be neutralized for DNA compaction (Bloomfield 1997). However, the experiments carried out by integral methods (e.g., by calorimetric analysis) indicated that DNA condensation proceeds at different degrees of neutralization of the charge of DNA phosphate groups, from 67% for cobalt hexamine to 87% for spermidine (Matulis et al. 2002). In addition, it was shown that the theoretical approach of Manning is a rather rough approximation of the Poisson-Boltzmann theory (Frank-Kamenetskii et al. 1987).

The surface of mica, a standard substrate for AFM, is negatively charged in buffer solutions at neutral pH values (Butt 1991). Therefore, the immobilization of negatively charged DNA molecules on the mica surface is carried out using several approaches that enable a change in the total negative surface charge of mica to the positive (Bezanilla et al. 1994; Lyubchenko and Shlyakhtenko 1997; Sato et al. 1999).

Mica can be modified by aminosilanes in both solution (in this case, self-associated monolayers of aminosilane molecules are formed on the surface of amino mica) (Fang and Hoh 1998b; Umemura et al. 2001) and in gas phase (Shlyakhtenko et al. 1999). In the first variant, the adsorbed DNA molecules are at a distance of about 1 nm from the mica surface (with the use of APTES) (Fang and Hoh 1998b). In the second variant, that is used in the present study, this distance is much more difficult to determine, because the structure of the surface layer of amino mica has been studied only by indirect methods. For example, an analysis of AFM images of structures such as spheroids and dimers compacted on the amino mica obtained in gas phase indicates that DNA molecules appear to be partially immersed into the surface layers of aminosilane. Adjacent to these structures with an increased density are always regions of amino mica in which the height of the aminosilane layer is substantially less than its height in the absence of spheroids or dimers.

The localization of DNA molecules immobilized on the surface of amino mica crucially differs from that on freshly cleaved mica (in the presence of  $Mg^{2+}$ ). In the first case, DNA molecules are at a much greater distance from the mica surface than upon adsorption onto mica coated

with  $Mg^{2+}$  ions. In addition, the “dip” of a DNA molecule in aminosilane layers on the mica surface provides, due to volume interactions, not only a stronger (compared with linear interactions in the case of freshly cleaved mica in the presence of  $Mg^{2+}$ ) shielding of negatively charged phosphate groups of DNA by positively charged amino groups exposed on the amino mica surface, but also a dynamic mobility of DNA molecules.

One of the substantial factors contributing to the compaction of scDNA may be intermolecular interactions that result in screening of negatively charged DNA phosphate groups by positively charged amino groups of modified amino mica (Limanskii 2000). This type of screening results in a decrease in the distance between base pairs along the duplex axis. The results presented here show that: i) compaction of single DNA molecules is possible *in vitro* without proteins, ii) a hydrophobicity and a high surface density of positively charged substrate is of crucial importance for the compaction and effective immobilization of scDNA.

It should be noted that freshly cleaved mica with a small negative surface charge significantly influences the amino group properties of APTES immobilized on the mica surface. It is noteworthy that the ionization constant (pK) of APTES in aqueous solution is  $\sim 10$  (Lyman's'kyy and Limans'ka 2003), but on the mica surface it is approximately 7 (Vezenov et al. 1997; Zhang et al. 1998). On the other hand, the pK of both APTES and nucleotides can be reduced under the influence of the mica surface properties. This means that nucleic acids bases can be protonated under the conditions used here (i.e. for DNA immobilization on the modified amino mica).

We visualized few unexpected molecules with net forming fragments (data not shown). One of reasons for the formation of these structures may be intramolecular triplexes (H-DNA). Sequence of pGEMEX DNA contains four fragments of 6 bp length that can form H-DNA (data are not shown). It is well known that H-DNA appears in purine/pyrimidine DNA sequences at pH  $\sim 4$  in aqueous solution, showing that a transition from B-DNA to H-DNA is possible by decreasing the pH 3 units from its physiological value (Lyamichev et al. 1987). The 3 pH units shifts to acidic values for the constant ionization of molecules immobilized on the freshly cleaved mica. A similar net of plasmid DNA molecules immobilized on the freshly cleaved mica was visualized in a narrow range of  $Mg^{2+}$  ion concentration (Wu et al. 2001). These results show that scDNA molecules form a net only within a small range of the surface charge density and DNA concentration.

There are additional factors of the observed DNA compaction. Quantum-chemical estimations (Kabanov and Komarov 2002; Kabanov et al. 2004) of the hydration influence on the structure of the short duplexes have shown a very strong role of a net of hydrogen bound water molecules for folding nucleotides pairs into the duplex. This results

in decreasing distances between nucleotides, transition of nucleotide pairs from one polymorphic form of H-pairing to another one. We suppose that effect of changing hydration environment of nucleotides in DNA can occur together with charge neutralization of phosphate groups upon DNA immobilization on the amino mica.

Several conclusions can be drawn from these results. The use of modified amino mica with the high surface charge density results in efficient compaction of scDNA molecules. For increased DNA superhelical density, there is reduced superhelical axis length contrary to a previous report that showed the length of the superhelical axis to be constant at 35% of the contour length of the relaxed molecule (Boles et al. 1990). Single DNA molecules with an extremely high level of compaction (rods, minitoroids, semispheroids, spheroids) were visualized on modified amino mica, characterized by increased hydrophobicity and surface charge density attributed to protonated amino groups. Contrary to previously reported multimolecular compaction of linear and scDNA molecules, we observed compaction for single scDNA molecules. The calculated apparent volume of scDNA molecules compared with the theoretical excluded volume of pGEMEX DNA allow for the discrimination of dimers and compacted structures formed from single scDNA molecules. A length of the molecules superhelical axis of the first order is decreased from ~570 to ~370 nm. At higher compaction levels, the superhelical axis shifts to second (~280 nm, 20% contour length of relaxed molecules) and third order (~140 nm, ~10% contour length of relaxed molecules). In other words, the two- or four time folding DNA takes place in two stages. The formation of minitoroids ( $d \sim 50$  nm) and molecules in the spherical conformation was the final stage of single molecule compaction. Cross-sectional profiles of minitoroid indicate that toroidal molecules may be formed from the bending of rod-like molecules. The proposed model for possible conformational transitions of scDNA *in vitro* and in the absence of proteins demonstrates that compaction of DNA dimers, trimers and single DNA molecules is possible if the substrate on which DNA molecules are immobilized has a high surface charge density and a hydrophobicity.

The screening of negatively charged DNA phosphate groups by positively charged protonated amino groups of the modified amino mica, allows for the following DNA molecular transitions: i) decreasing the distance between nucleotides along the duplex axis and the formation of S-DNA (reduced helical rise/bp), ii) the formation of H-DNA (intramolecular triplexes). Our experimental data are consistent with an increased flexibility of DNA following immobilization onto a positively charged surface as predicted by G. Manning's theory (Manning 1978) and found experimentally (Podesta et al. 2005). Based on the analysis of AFM images for scDNA molecules, we suggest that immobilization of the scDNA on the modified amino mica provides a good model for proc-

esses to mimic DNA folding *in vivo*. DNA in the eukaryotic nucleus and in the nucleoid of bacterial cell is located in a medium with a high density of charged moieties comprised of different molecules such as proteins, polysaccharides, and lipids. An insignificant number of scDNA (~3%) and semispheroids (~4%) were observed compared with the number of spheroids (~17%) implies that semispheroids are intermediate forms during compaction of scDNA up to the level of spheroids.

**Acknowledgements.** This work was supported by grant AMS 72/2007 from Ukrainian Academy of Medical Sciences. We thank Dr. A. Sivolob (Kiev National University, Ukraine) and Dr. A. Shestopalova (Institute of Radiophysics and Electronics of UAS, Ukraine) for critical reading of the manuscript and useful discussions. We wish to thank anonymous referees for thorough reading of the manuscript and their constructive comments.

## References

- Allen M., Bradbary E., Balhorn R. (1997): AFM analysis of DNA-protamine complexes bound to mica. *Nucleic Acids Res.* **25**, 2221–2226
- Anderson C., Record M. (1995): Salt-nucleic acid interactions. *Annu. Rev. Phys. Chem.* **46**, 657–700
- Bezanilla M., Drake B., Nudler E., Kashlev M., Hansma P., Hansma H. (1994): Motion and enzymatic degradation of DNA in the atomic force microscope. *Biophys. J.* **67**, 2454–2459
- Bloomfield V. (1997): DNA condensation by multivalent cations. *Biopolymers* **44**, 269–282
- Boles T., White J., Cozzarelli N. (1990): Structure of plectonemically supercoiled DNA. *J. Mol. Biol.* **213**, 931–951
- Brodsky L., Drachev A., Leontovich A. (1991): Package of applied programs for biopolymers sequences analysis: GeneBee. *Biopolimery i Kletka*, **7**, 10–14 (in Russian)
- Butt H. (1991): Measuring electrostatic, van der Waals, and hydration forces in electrolyte solutions with an atomic force microscope. *Biophys. J.* **60**, 1438–1444
- Bussiek M., Mucke N., Langowski J. (2003): Polylysine-coated mica can be used to observe systematic changes in the supercoiled DNA conformation by scanning force microscopy in solution. *Nucleic Acids Res.* **31**, 1–10
- Cherny D., Jovin T. (2001): Electron and scanning force microscopy studies of alterations in supercoiled DNA tertiary structure. *J. Mol. Biol.* **313**, 295–307
- Dunlap D., Maggi A., Soria M., Monaco L. (1997): Nanoscopic structure of DNA condensed for gene delivery. *Nucleic Acids Res.* **25**, 3095–3101
- Fang Y., Hoh J. (1998a): Surface-directed DNA condensation in the absence of soluble multivalent cations. *Nucleic Acids Res.* **26**, 588–593
- Fang Y., Hoh J. H. (1998b): Early intermediates in spermidine-induced DNA condensation on the surface of mica. *J. Am. Chem. Soc.* **120**, 8903–8909
- Fang Y., Hoh J. (1999): Cationic silanes stabilize intermediates in DNA condensation. *FEBS Lett.* **459**, 173–176

- Frank-Kamenetskii M. D., Anshelevich V. V., Lukashin A. V. (1987): Polyelectrolyte model of DNA. *Usp. Fiz. Nauk* **151**, 595–618 (in Russian)
- Golan R., Pietrasanta L., Hsieh W., Hansma H. (1999): DNA toroids: stages in condensation. *Biochemistry* **38**, 14069–14076
- Gonzalez-Huici V., Salas M., Hermoso J. (2004): Genome wide, supercoiling-dependent *in vivo* binding of a viral protein involved in DNA replication and transcriptional control. *Nucleic Acids Res.* **32**, 2306–2314
- Grosberg A., Khokhlov A. (1989): *Statistical Physics of Macromolecules*. Nauka Publishers, Moscow (in Russian)
- Hansma H., Golan R., Hsieh W., Lollo C., Mullen-Ley P., Kwoh D. (1998): DNA condensation for gene therapy as monitored by atomic force microscopy. *Nucleic Acids Res.* **26**, 2481–2487
- Hizume K., Yoshimura S., Maruyama H., Kim J., Wada H., Takeyasu K. (2002): Chromatin reconstitution: development of a salt-dialysis method monitored by nano-technology. *Arch. Histol. Cytol.* **65**, 405–413
- Hud N., Downing K. (2001): cryoelectron microscopy of  $\lambda$  phage DNA condensates in vitreous ice: the fine structure of DNA toroids. *Proc. Natl. Acad. Sci. U.S.A.* **98**, 14925–14930
- Kabanov A., Komarov V. (2002): Polymorphism of hydrogen bonding in the short double helices of oligonucleotides. Quantum-chemical semiempirical study. *Int. J. Quantum Chem.* **88**, 579–587
- Kabanov A., Komarov V., Yakushevich L., Teplukhin A. (2004): Low-frequency intra- and intermolecular vibration modes of H-bonded nucleobases in oligonucleotide double helices and hydrated nucleotide duplex: application of the PM3 method. *Int. J. Quantum Chem.* **100**, 595–609
- Kemura K., Rybenkov V., Crison N., Hirano T., Cozzarelli N. (1999): 13S condensin actively reconfigures DNA by introducing global positive writhe: implications for chromosome condensation. *Cell* **98**, 239–248
- Kim J., Yoshimura S., Hizume K., Ohniwa R., Ishihama A., Takeyasu K. (2004): Fundamental structural units of the *Escherichia coli* nucleoid revealed by atomic force microscopy. *Nucleic Acids Res.* **32**, 1982–1992
- Korolev N., Lyubartsev A., Laaksonen A., Nordenskiöld L. (2003): A molecular dynamics simulation study of oriented DNA with polyamine and sodium counterions: diffusion and averaged binding of water and cations. *Nucleic Acids Res.* **31**, 5971–5981
- Limanskii A. (2000): Visualization of cruciform structure in supercoiled DNA by atomic force microscopy. *Biofizika* **45**, 1039–1043 (in Russian)
- Limansky A. P., Shlyakhtenko L. S., Schaus S., Henderson E., Lyubchenko Y. L. (2002): Aminomodified probes for atomic force microscopy. *Probe Microscopy* **2**, 227–234
- Lin C., Wang C., Feng X., Liu M., Bai C. (1998): The observation of the local ordering characteristics of spermidine-condensed DNA: atomic force microscopy and polarizing microscopy studies. *Nucleic Acids Res.* **26**, 3228–3234
- Lyamichev V., Mirkin S., Frank-Kamenetskii M. (1987): Structure of  $(dG)_n \cdot (dC)_n$  under superhelical stress and acid pH. *J. Biomol. Struct. Dyn.* **5**, 275–282
- Lyubchenko Y., Shlyakhtenko L. (1997): Visualization of supercoiled DNA with atomic force microscopy *in situ*. *Proc. Natl. Acad. Sci. U.S.A.* **94**, 496–501
- Lymans'kiy A. P., Lymans'ka O. Yu. (2002): Study of microorganisms genome DNA by atomic force microscopy. *Tsitol. Genet.* **36**, 30–36 (in Russian)
- Lymans'kiy A. P., Limans'ka O. Yu. (2003): Visualization of cyanobacteria in aqueous solution by atomic force microscopy. *Tsitol. Genet.* **37**, 68–71 (in Russian)
- Manning G. (1978): The molecular theory of polyelectrolyte solutions with application of the electrostatic properties of polynucleotides. *Q. Rev. Biophys.* **11**, 179–246
- Martinkina L., Kolesnikov A., Streltsov S., Yurchenko V., Vengerov Y. (1998): Circular superhelical DNA complexes with synthetic oligopeptide: unusual compact structures and influence of bent sequences on the results of compaction. *J. Biomol. Struct. Dyn.* **15**, 949–957
- Martinkina L., Klinov D., Kolesnikov A., Yurchenko V., Streltsov S., Neretina T., Demin V., Vengerov Y. (2000): Atomic force and electron microscopy of high molecular weight circular DNA complexes with synthetic oligopeptide trivalentine. *J. Biomol. Struct. Dyn.* **17**, 687–695
- Matulis D., Rouzina I., Bloomfield V. (2002): Thermodynamics of cationic lipid binding to DNA and DNA condensation: roles of electrostatics and hydrophobicity. *J. Am. Chem. Soc.* **124**, 7331–7342
- Morgan J., Blankenship J., Mattheus H. (1987): Polyamines and acetylpolyamines increase the stability and alter the conformation of nucleosome core particles. *Biochemistry* **26**, 3643–3649
- Podesta A., Indrieri M., Brogioli D., Manning G., Milani P., Guerra R., Finzi L., Dunlap D. (2005): Positively charged surfaces increase the flexibility of DNA. *Biophys. J.* **89**, 2558–2563
- Polyanichko A., Chikhirzhina E., Andrushenko V., Kostyleva E., Weiser H., Vorob'ev V. (2002): The effect of  $Ca^{2+}$  ions on DNA compaction in the complex with non-histone chromosomal protein HMGB1. *Mol. Biol. (Moskva)* **38**, 701–712 (in Russian)
- Reiner C., Stroh C., Ebner A., Klampfl C., Gall A., Romanin C., Lyubchenko Y., Hinterdorfer P., Gruber H. (2003): Simple test system for single molecule recognition force microscopy. *Analyt. Chim. Acta* **479**, 59–75
- Rivetti C., Codeluppi S., Dieci G., Bustamante C. (2003): Visualizing RNA extrusion and DNA wrapping in transcription elongation complexes of bacteria and eukaryotic RNA polymerases. *J. Mol. Biol.* **326**, 1413–1426
- Saenger W. (1984): *Principles of Nucleic Acids Structure*. Springer, New York
- Sato M., Ura K., Hohmura K., Tokumasu F., Yoshimura S., Hanaoka F., Takeyasu K. (1999): Atomic force microscopy sees nucleosome positioning and histone H1-induced compaction in reconstituted chromatin. *FEBS Lett.* **452**, 267–271
- Sivolob A., Prunell A. (2004): Nucleosome conformational flexibility and implications for chromatin dynamics. *Philos. Trans. R. Soc. London, Ser. A.* **362**, 1519–1547
- Shlyakhtenko L., Gall A., Weimer J., Hawn D., Lyubchenko Y. (1999): Atomic force microscopy imaging of DNA cova-

- lently immobilized on a functionalized mica substrate. *Biophys. J.* **77**, 568–576
- Tanigawa M., Okada T. (1998): Atomic force microscopy of supercoiled DNA structure on mica. *Anal. Chim. Acta* **365**, 19–25
- Umemura K., Ishikawa M., Kuroda R. (2001): Controlled immobilization of DNA molecules using chemical modification of mica surfaces for atomic force microscopy: characterization in air. *Anal. Biochem.* **290**, 232–237
- Vezenov D., Noy A., Rozsnyai L., Lieber C. (1997): Force titrations and ionization state sensitive imaging of functional groups in aqueous solutions by chemical force microscopy. *J. Am. Chem. Soc.* **119**, 2006–2015
- Wu A., Li Z., Yu L., Wang H., Wang E. (2001): Plasmid DNA network on a mica substrate investigated by atomic force microscopy. *Anal. Sci.* **17**, 583–584
- Yoshimura S., Hizume K., Murakami A., Sutani T., Takeyasu K., Yanagida M. (2002): Condensin architecture and interaction with DNA: regulatory non-SMC subunits bind to the head of SMC heterodimer. *Curr. Biol.* **12**, 508–513
- Zhang H., He H., Wang J., Mu T., Liu Z. (1998): Force titration of amino group-terminated self-assembled monolayers using chemical force microscopy. *Appl. Phys. A: Solids Surf.* **66**, S269–271
- Zinchenko A., Yoshikawa K. (2005): Na<sup>+</sup> shows a markedly higher potential than K<sup>+</sup> in DNA compaction in a crowded environment. *Biophys. J.* **88**, 4118–4123
- Zimmerman S. B. (2004): Studies on the compaction of isolated nucleoids from *Escherichia coli*. *J. Struct. Biol.* **147**, 146–158

Received: April 15, 2008

Final version accepted: September 3, 2008